Check for updates

Silver nanoparticle from whole cells of the fungi *Trichoderma* spp. isolated from Brazilian Amazon

Matheus M. Ramos · Edmilson dos S. Morais · Iracirema da S. Sena ·
Adilson L. Lima · Fábio R. de Oliveira · Calleu M. de Freitas · Caio P. Fernandes ·
José Carlos T. de Carvalho · Irlon M. Ferreira

Abstract Metal nanoparticles are a promising approach for the development of new antimicrobial systems. Silver nanoparticles (AgNP) have a significant antibacterial activity through bacterial surface adsorption and oxidative stress induction, as indicated by recent observations. This research aimed to use endophytic fungi from the genus *Trichoderma* spp. isolated from the *Bertholletia excelsa* (Brazil-nut) seeds and the soil to biosynthesize AgNPs and also test their antibacterial activity. The use of these fungi for this purpose not only valorizes the Amazon biodiversity but it also uses cleaner and cheaper processes, being part of the Green Chemistry concept. The particles were analyzed through Ultraviolet–Visible Spectroscopy and ZetaSizer and the band of absorption at 420 nm was analyzed through Localized Surface Plasmon Resonance. After characterization, the AgNP were tested for antibacterial activity against several bacterial strains, when it was observed that their antibacterial activity was superior in Gram-negative bacteria.

M. M. Ramos · E. dos S. Morais · I. da S. Sena · I. M. Ferreira (✉)
Laboratório de Biocatálise e Síntese Orgânica Aplicada, Departamento de Ciências Exatas, Universidade Federal do Amapá, Rod. JK, KM 02, Macapá, Amapá 68902-280, Brazil
e-mail: irlon.ferreira@gmail.com

A. L. Lima
Controle Biológico, Empresa Brasileira de Pesquisa Agropecuária (Embrapa), Macapá, Amapá, Brazil

F. R. de Oliveira · C. M. de Freitas
Laboratório de Controle de Qualidade e Bromatologia, Departamento de Ciências Biológicas e da Saúde, Colegiado de Farmácia, Universidade Federal do Amapá, Macapá, Amapá, Brazil

C. P. Fernandes
Laboratório de Nanobiotecnologia Fitofarmacêutica, Departamento de Ciências Biológicas e da Saúde, Colegiado de Farmácia, Universidade Federal do Amapá, Macapá, Amapá, Brazil

J. C. T. de Carvalho
Laboratório de Pesquisa em Fármacos, Departamento de Ciências Biológicas e da Saúde, Colegiado de Farmácia, Universidade Federal do Amapá, Macapá, Amapá, Brazil

Graphic abstract
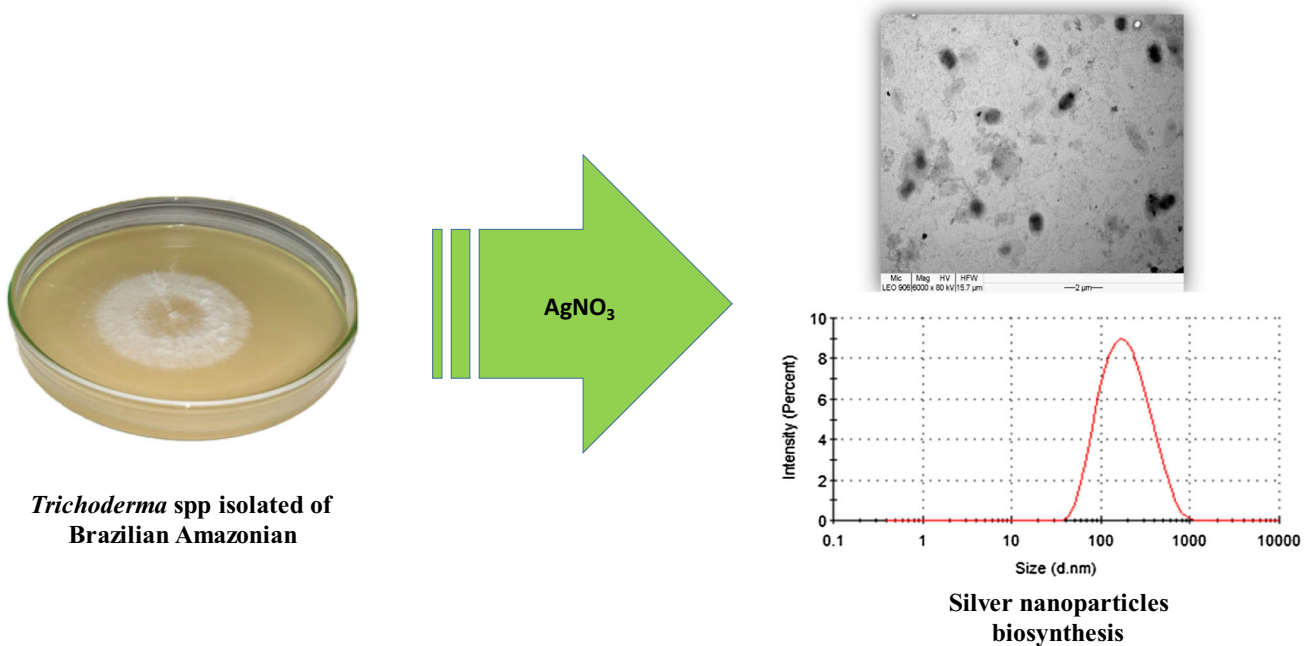
Trichoderma spp isolated of Brazilian Amazonian

AgNO₃ → **Silver nanoparticles biosynthesis**

Introduction

Silver nanoparticles (AgNP) can be obtained by chemical, physical and biological methods (Ko and Huh 2019; Ghiuţă et al. 2017). Chemical methods include chemical reduction, electrochemical methods and pyrolysis. However, most chemical methods need strong reducing agents such as borohydride and hydrazine derivatives, it can increase the process cost and the environmental impact due to the wastes (Edwards 2017; Liu and Jiang 2015). Physical methods (laser irradiation, vapor condensation) are less toxic than chemical methods; they are usually faster and produce more uniform particles (Ilaria and Kenny 2013; Welles 2010). However, a large amount of energy associated to the high costs may be a disadvantage of those methods. Biological methods use living organisms or their metabolites for synthesis; these methods are more advantageous since they do not handle toxic reagents and produce more

stable nanoparticles too (Balakrishnan 2014; Wei et al. 2015).

The biological agents used are *Lactobacillus*, *Escherichia coli*, fungi such as *Fusarium oxysporum* and *Ganoderma neo-japonicum*, plant extracts such as *Allophylus cobbe* and *Artemisia princeps* (Zhang et al. 2016). Among the major advantages of biological methods, it is possible to list biomolecules such as amino acids, proteins and secondary metabolites found in the reaction medium present on the aggregation of nanoparticles, in addition, AgNP synthesized by biological methods usually have more uniform shape and size compared to other methods (Neethu et al. 2018).

In a research published by Mishra et al. (2014), the fungus *Trichoderma viride* was able to produce gold nanoparticles with bactericidal activity against *Pseudomonas syringae*, *Escherichia coli*, *Shigella sonnei*. In other study, the filamentous fungus *T. harzianum* was able to produce AgNP with bactericidal activity against strains of *Staphylococcus aureus* and *Klebsiella pneumoniae* (Ahluwalia et al. 2014). The bactericidal activity of AgNP biosynthesized by *T. viride* was efficient against Gram-positive (*Staphylococcus aureus* Methicillin-Resistant—MRSA) and Gram-negative pathogens (*Shigella boydii*,

Acinetobacter baumannii, *Shigella sonnei,* and *Salmonella typhimurium*) using the agar diffusion method. Such particles were polydisperse with sizes ranging between 1 and 50 nm and the results showed that they had significant antibacterial activity against all the bacteria tested, especially against Gram-negative bacteria (Elgorban et al. 2016).

The Amazon soil has excellent potential for the isolation of new fungi species due to the high deposition of organic residues in the soil surface, which facilitates the collection process (Kelly et al. 2017). These organic residues under constant moisture provide the ideal substrate for the proliferation of microorganisms in decomposition such as bacteria and fungi (Pathma and Sakthivel 2012). However, there is currently insufficient information available about the Amazon microbiota and its pharmacological and biotechnological potential since the Amazon Forest is the most biodiverse ecosystem in the world (Hargreaves and Pereira 2008).

In this sense, this study aimed to use fungi from the genus *Trichoderma* spp. isolated from the soil and *Bertholletia excelsa* (Brazil nut) seeds to synthesize AgNP. Considering the available data in the literature on the genus *Trichoderma* spp., it is expected that such Amazon fungi would be able to produce AgNP with potential anti-bacterial activity. This work is one of the pioneers on bioprospecting Amazon fungal isolates for AgNP production. In addition, the emergence of antibiotic resistant bacteria has become a worldwide health problem and AgNP are presented as an alternative for the improvement of existing antibiotics in the market, as their association with antimicrobials generates products with a broader spectrum of action and power (McShan et al. 2015). The possibility of synthesizing AgNP in an ecologically correct and less expensive way enhances the Amazon biotechnological potential and encourages technological development in the region.

Experimental

Reagents and solution

The salt $AgNO_3$ (> 99%) and DMSO (99%) were purchased from Synth. The salts NaH_2PO_4 and K_2HPO_4 used to prepare the phosphate buffer solution, as well as NaOH (99%) and HCl (37%) were obtained

from Vetec. Malt extract, Agar Muller Hinton and Nutrient broth obtained from HiMedia RM004B. The syringe water was purchased from Farmace®.

Trichoderma spp. fungi isolation

The 04 (four) isolates used in this study were obtained from soil and endocarps of *Bertholletia excelsa* (Brazil nut) (Table 1). Malt extract (2%) plus chloramphenicol were used to obtain the isolates. To obtain the isolates from the soil was performed the serial dilution technique; the isolates obtained from Brazil nut endocarps were obtained by scraping of the surface. After isolation, the Petri dishes containing the isolates were transferred to a B.O.D. incubator using 12 h photoperiod at 26 ± 1 °C. After seven days of incubation, the colonies of morphological structures (conidiophores and conidia) were analyzed to identify the fungi at the genus level according to Holanda et al. (2019).

Fungi cultivation on solid medium

The strains used in this work were provided by EMBRAPA (Empresa Brasileira de Pesquisa Agropecuária). All fungi used were from the genus *Trichoderma*, and the methodology used, for the culture on solid medium was proposed by Birolli et al. (2017): 2.0 g of malt extract and 2.0 g of agar solubilized in 100 mL of distilled water. The pH was adjusted to 7.0 using 0.1 M KOH or HCl solution and the resulting liquid medium was autoclaved for 20 min at 121 °C. The resulting solution was poured into Petri dish (9 cm) and after solidification of the medium, the fungi were skinned. Finally, the plates stayed in incubator B.O.D. for 7 days at 32 °C, allowing the fungi to grow.

Fungi cultivation in liquid medium

The fungi inoculation in liquid medium was performed in a sterile environment by transferring four circular fragments of the solid medium (0.5 cm in diameter) with the mycelia from the stock culture. The microbial growth was performed with 100 mL of culture medium containing 2% of malt extract and distilled water in an Erlenmeyer flask (250 mL) closed with a cotton plug. The pH of the solution was adjusted to 7.0 with 0.1 M KOH solution or 0.5 M HCl. The

flask was kept under rotary shaking for 9 days (28 ± 2 °C, 130 rpm). After this period, the fungal mycelia were separated from the liquid medium through vacuum filtration using Whatman no 1 filter paper and then washed 3 times with autoclaved distilled water (Ferreira et al. 2015).

AgNP biosynthesis

In order to obtain AgNP, it was used an adapted method based on Gaikwad et al. (2013). The mycelia from isolates *Trichoderma* spp. grown in liquid medium were filtered and 2.0 g of wet mass was transferred, in a sterile environment, to Erlenmeyer flasks (250 mL) by containing 100 mL of $AgNO_3$ solution at 1.0 mmol/L. The flasks were kept under orbital shaking within a temperature-controlled (32 °C) shaker incubator (Luca-222, Lucadema) away from the light. The medium containing the filamentous fungi was kept in contact with the $AgNO_3$ solution for 9 days under orbital agitation. It is important to emphasize that all experiments were performed three times and after this period, the content of each flask was vacuum filtered on Büchner funnel, the mycelial masses were discarded and the resulting solutions were subjected to UV–Vis spectroscopic analysis (Thermo Scientific, Genesys 10 UV) and ZetaSizer analysis (Malvern Instruments Corp, Nano—ZS). The best isolate *Trichoderma* spp. was chosen based on the following parameters: RPSL band intensity at 420 nm, smaller average hydrodynamic size, zeta potential and smaller polydispersity index.

AgNP optimization synthesis

The isolate TCH 01 was subjected to optimization tests to decrease the AgNPs average size. In this way, were performed tests of pH variation (5, 6 and 7) and reaction time (3, 6, 9 and 12 days) by following the procedure described in item 2.5.

AgNP characterization

The solution containing AgNP after vacuum filtration was centrifuged at 4000 rpm for 10 min. The precipitate was re-suspended in 10 mL of syringe water and vortexed (1000 rpm for 2 min) to analyze 2 mL of the resulting solution.

Ultraviolet–visible spectroscopy (UV–Vis)

In this analysis, the $AgNO_3$ solution was subjected to orbital agitation with the mycelia and then centrifuged at 4000 rpm for 10 min in EDUTEC, TD4N model centrifuge. After that procedure, the supernatant was partially discarded until just 5 mL left. The precipitate was resuspended in the remaining 5 mL of supernatant and the resulting solution was further characterized. The formation of AgNP was confirmed by the presence of the plasmon resonance band, analyzed through an UV–Vis spectrophotometer (Thermo Scientific, Genesys 10 UV) with a resolution of 1 nm and a wavelength of 200–500 nm.

ZetaSizer

To analyze the hydrodynamic particle diameter, zeta potential, PDI and temperature variation was used ZetaSizer equipment (Malvern Instruments Corp., Nano ZS). After orbital agitation with the fungal mycelia, the $AgNO_3$ solutions were vortexed (KASVI, K45-2820) for 2 min; then the surface charges obtained from nanoparticles in a liquid medium, their average hydrodynamic size and polydispersity index were measured in 10 mm thick quartz cuvettes.

Fourier transform infrared spectroscopy (FTIR)

The Infrared spectra (FTIR) were obtained on a PerkinElmer—Spectrum Two (U.S.A.) spectrometer by operating with Fourier Transform and ATR (Attenuated Total Reflectance) accessory. The spectra were obtained in the region of 4.000 to 400 cm^{-1}, accommodating the sample previously concentrated after 10 min of centrifugation at 4.000 rpm (EDUTEC centrifuge, TD4N) and with discarded supernatant. It should be noted that the precipitate was placed in direct contact with the ATR.

In vitro antibacterial activity

The antibacterial activity was evaluated against the following standard strains: (i) Gram-positive bacteria: *Staphylococcus aureus* (ATCC 6538) and *Enterococcus faecalis* (ATCC 29,212); (ii) Gram-negative bacteria: *Pseudomonas aeruginosa* (ATCC25853), *Escherichia coli* (ATCC 8739). All strains were obtained from INCQS/FIOCRUZ.

Table 1 Municipalities of fungi collection

Isolate	Substrate	Municipalities	Species
TCH-01	Soil	Macapá, AP	*Trichoderma* sp.
TCH-02	Chestnut endocarp	Laranjal do Jari, AP	*Trichoderma* sp.
TCH-03	Chestnut endocarp	Laranjal do Jari, AP	*Trichoderma* sp.
TCH-06	Soil	Macapá, AP	*Trichoderma* sp.

To prepare the bacterial inoculum, the strains were 24 h cultured in Muller Hinton Agar (MHA) for 18 h at 37 °C and lead to exponential phase in Mueller–Hinton (MH) broth at 37 °C for 1 h. The turbidity was adjusted to 0.5 on the McFarland scale (about 2×10^8 CFU/mL) by dilution of new cultures and then diluted to 1×10^3 CFU/mL as described by the Clinical and Laboratory Standards Institute (CLSI 2012).

Determination of the minimum inhibitory concentration (MIC) and minimum bactericidal concentration (MBC) of AgNP

MIC is defined as the lowest concentration of a fraction that inhibits the microorganism growth. The AgNP dispersions were dissolved in a 10% dimethyl-sulfoxide (DMSO) solution and adjusted to a concentration of 5 mg/mL in MH broth and serially diluted until the concentrations used in the tests were obtained (2.5, 1.25, 0.62, 0.31, 0.15, and 0.07 mg/mL). For the microdilution test, 100 μL of the inoculum containing 1×10^3 CFU/mL was added to each well and 100 μL of serial dilutions were transferred to consecutive wells. After 24 h of incubation, 30 μL of 0.01% resazurin (phenoxazine-3-one) was added to the wells to allow visual identification of metabolic activity. After incubation for 3 h at 37 °C, the growth was indicated by the appearance of a pink color. MIC was read as the lowest AgNP concentration where occurred color change. MBC determination, 10 μL of each well content were withdrawn and incubated in MHA at 37 °C for 24 h. MBC was defined as the lowest concentration of AgNP that resulted in no growth or less than three colonies (99.9% death). Each test was performed in triplicates. The negative control consisted of 100 μL of the bacterial inoculum in 100 μL of DMSO. Chloramphenicol (50 mg/mL) and gentamicin (10 mg/mL) were used as positive controls for Gram-positive and Gram-negative bacteria, respectively.

Results and discussion

Screening of the *Trichoderma* spp. isolates

From the four strains of *Trichoderma* spp. used, the strain TCH 01 (Fig. 1a) reported the best results. It was observed that after nine days, the reaction medium containing AgNP solution and the isolate TCH 01 changed from transparent to a brown color (Fig. 1b). Such coloration may indicate the presence of Localized Surface Plasmon Resonance (LSPR) observed at 420 nm in the UV–Vis spectrum (Fig. 2a) (Ravindran et al. 2013). Moreover, the strain TCH 01 reported the smallest particles (261 nm) during the screening (Fig. 2b), and consequently, has been chosen for the other tests.

Is possible to see the values of polydispersity index (PDI) in Fig. 3. This parameter is an indicator from the homogeneity of the size distribution; the smaller the PDIthe more homogeneous are the particles diameters (Cardoso 2017). Besides TCH 01, any other isolate had the presence of LSPR band between at 400 and 450 nm in UV–Vis spectroscopy; it is that so because of the different geometrical shapes since few differences in a particle geometry can result in significant changes of LSPR peaks in metallic nanoparticles, also, the THC 01 demonstrated potential for AgNP production, probably due to the high production of redox enzymes. However, during screening, the fungus with the smallest average hydrodynamic particle size and LSPR band in the UV–Vis spectrum was prioritized. The adsorption of molecules from the reaction medium in specific areas can impair or increase the nanoparticles growth toward different directions. In some instances, the formation of surfactant micelles can physically direct the anisotropic growth (Sajanlal et al. 2011).

The zeta potential relies on the charge of the particles surface charge; it is directly affected by the medium where the particles are dispersed and reasonable stability is achieved after ± 30 mV. The isolate

Fig. 1 a *Trichoderma* sp. TCH 01 in solid medium (malt and agar 2%, 7 days, 32 °C. **b** Flasks with TCH 01 solutions; 1—control AgNO$_3$ solution; 2—fungi solution without AgNO$_3$; fungi + AgNO$_3$ solution
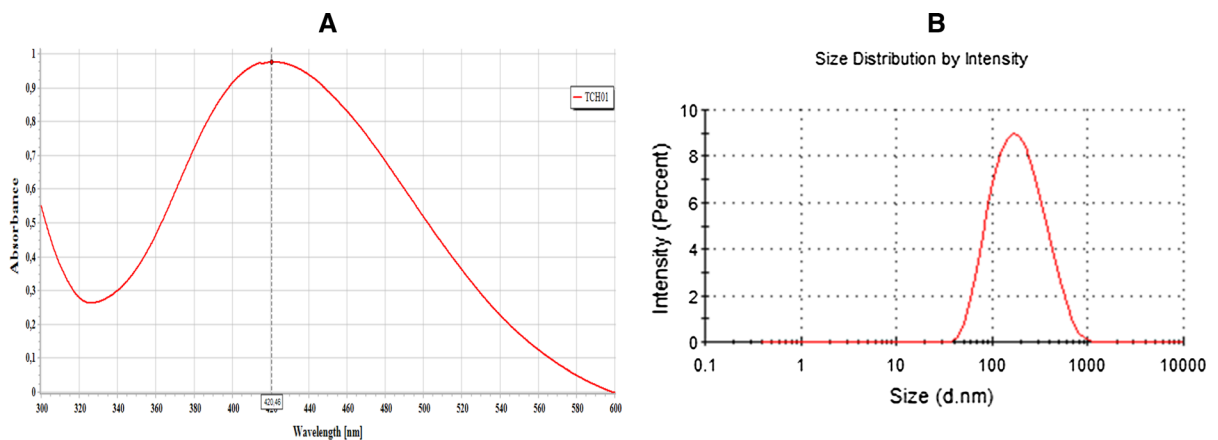

Fig. 2 a UV–Vis spectrum of AgNP solution from *Trichoderma* sp. TCH 01. **b** AgNP size distribution

TCH 02 had the best zeta potential, followed by TCH 06, TCH 01 and TCH 03 (Fig. 3). The closer to zero is the zeta potential the higher the tendency of particles agglomeration, on this research, all the dispersions had a fairly low zeta potential, with values ranging between − 15 and − 23 mV. However, this parameter is not the only one determining a colloid stability since they can be stable even with a low zeta potential (Cavalcante 2014).

Figures 4a, b show a directly proportional relationship between decreased pH and decreased particles hydrodynamic size, as the growth of TCH 01 in basic medium (pH 8) resulted in the formation of particles with 260 nm, while in pH 5 resulted in particles with 160 nm. The ideal pH of fungi growth is often between 4.0 and 6.0; however, filamentous fungi tolerate variations ranging from 2.0 to 9.0 (Marinho et al. 2017). In low pH, some fungi are stimulated to

produce higher quantities of metabolites, besides key enzymes that will oxidize the nitrate of the reaction medium, with consequent formation of atomic silver. The overproduction of enzymes and metabolites under reduced pH in some fungi species can explain smaller-sized AgNP when cultivated in acid pH (Chen et al. 2015).

The zeta potential varied according to the pH, ranging between − 14 and − 15 mV (in TCH 01 medium grown in pH 5, 6, and 8) and between − 19 and − 20 mV (in TCH 01 medium grown in pH 7), as shown in Fig. 4a. According to the literature, the presence of ions or negatively charged molecules in the medium decreases the zeta potential of particles surface, and conversely, positively charged ions increase the zeta potential. Proteins in the medium can increase the nanoparticles stability after dispersion; on the other hand, proteins can induce particles
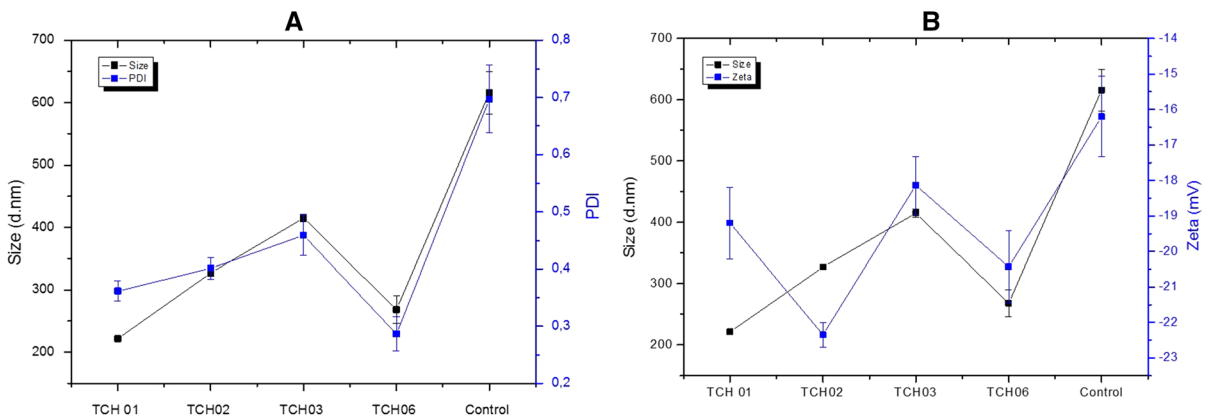
Fig. 3 **a** Nanoparticles from *Trichoderma* sp. TCH 01 average hydrodynamic size and zeta potential. **b** Average hydrodynamic size and polydispersity index (PDI)
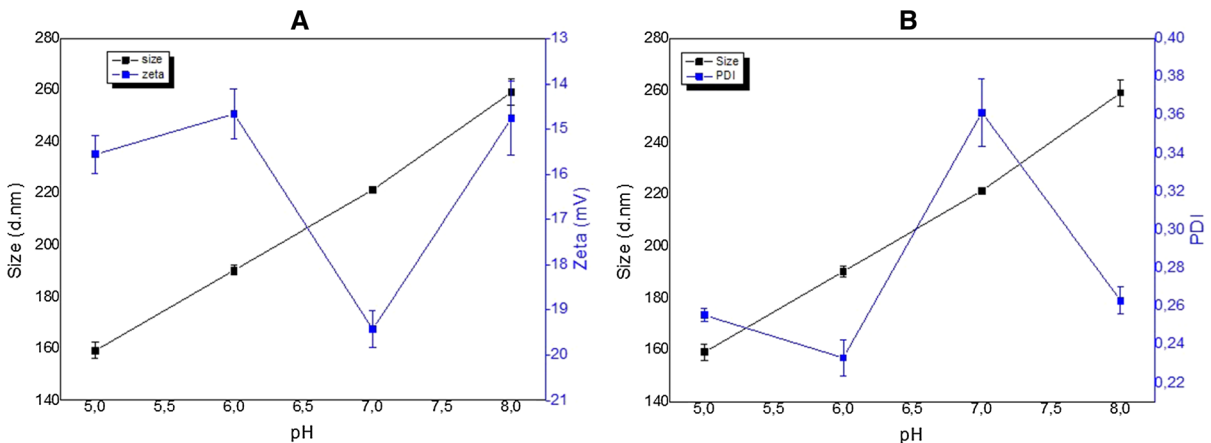

Fig. 4 **a** Influence of the pH over particles average hydrodynamic size and zeta potential. **b** Influence of the pH over particles average hydrodynamic size and polydispersity index (PDI)

agglomeration due to adsorption towards their surface, wich means, the presence of ions and proteins in the reaction medium at different concentrations can explain the oscillation of zeta potential observed in this study (Mikolajczyk et al. 2015). In Fig. 4b, it is seen that although the isolate grown in pH 6 has a lower PDI (0.233), this isolate had bigger particles size (190 nm), and consequently, the isolate cultivated in pH 5 had AgNP with the best antibacterial features (Durán et al. 2016) and was further appraised.

Figure 5a shows diameter changes in the particles synthesized by TCH 01 over the time (3, 6, 9 and 12 days; pH 5). It can be seen a steady decrease in size until the 9th day (150 nm). The PDI at this day was also adequate: 0.283 (Fig. 5b) the AgNP synthesized

over 9 days (pH 5) had the best physical features for antibacterial activity. On the 12th day the diameter reached 200 nm; this increase of diameter has already been reported as a consequence of long reaction periods since, after a certain period, the fungi reach a limit of synthesis and the particles already formed tend to aggregate. The zeta potential of these particles was about -10 to -15 mV, which indicates low stability of the dispersion and little influence of the period of reaction in this parameter (Shah et al. 2015).

Figure 6 shows the FTIR spectrum of TCH 01 medium (9 days, pH 5), where it is possible to see transmittance bands at 3400, 1650, 1290, 1219, 641 and 600 cm^{-1}. The band at 3400 cm^{-1} can be attributed to O–H groups from water, the bands at
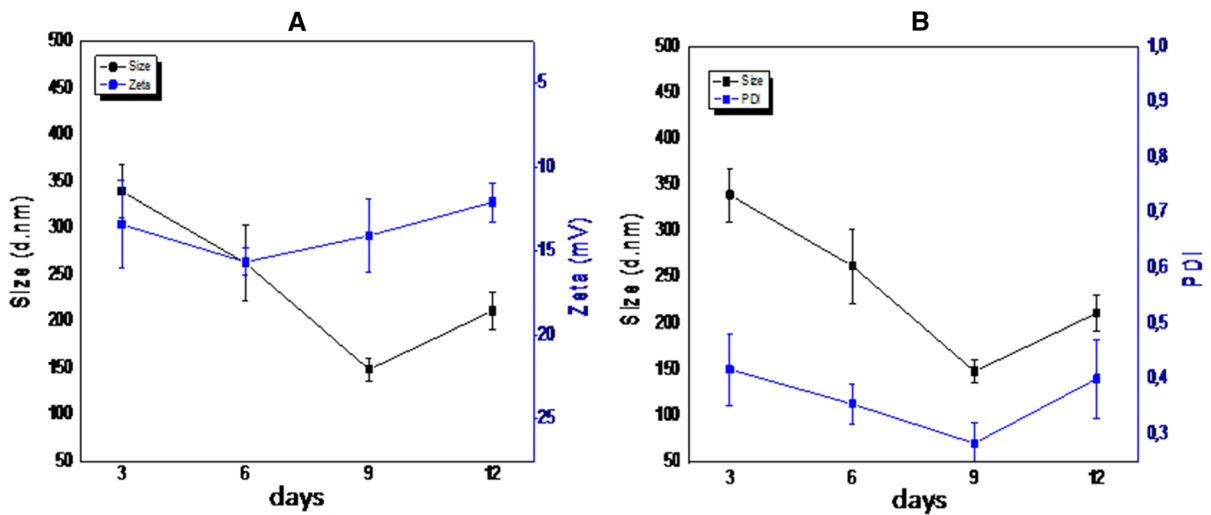
Fig. 5 **a** Influence of the time of reaction (days) over particles average hydrodynamic size and zeta potential from *Trichoderma* sp. TCH 01. **b** Influence of the time of reaction over particles average hydrodynamic size and polydispersity index (PDI)
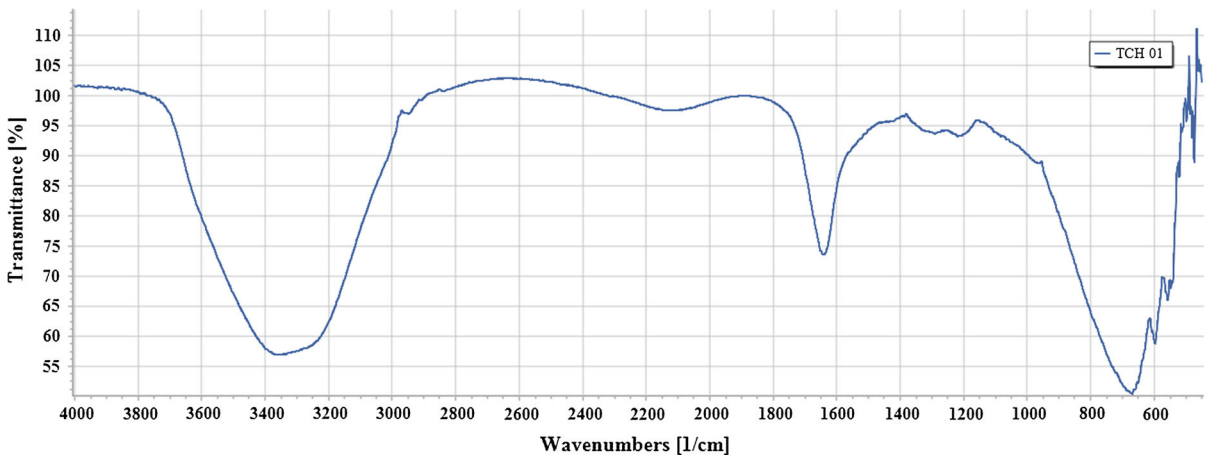

Fig. 6 FTIR spectrum of the reaction medium (AgNO₃ *Trichoderma* sp. TCH 01) after 9 days in pH 5

1290 and 1219 cm^{-1} can be attributed to remnant NO$_3$ found in the sample and the bands at 641 and 600 cm^{-1} indicate C–H bonds from aromatic rings (Almeida 2017). The presence of aromatic groups in the fungi medium can be due to the presence of aromatic amino acids such as tyrosine and tryptophan. Some proteins excreted by the fungi during AgNP biosynthesis can bond to them through free amine groups, cysteine residues or electrostatic attraction of negatively charged carboxylate groups. These findings suggest that the liberation of extracellular protein molecules possibly has a role in the formation and stabilization of the AgNP from the fungi medium.
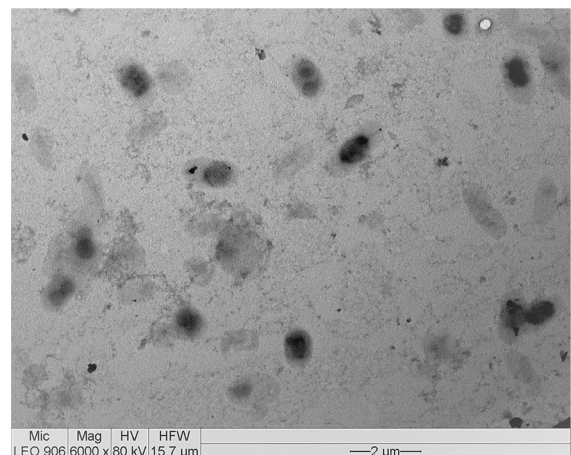

Fig. 7 TEM images of AgNP from *Trichoderma* sp. TCH 01

Table 2 Minimum inhibitory concentration (MIC) and minimum bactericidal concentration (MBC) from AgNP biosynthesized from TCH 01 (pH 5)

Mediums (days)	Bacteria—MIC and MBC (mg/mL)							
	Gram-positive				Gram-negative			
	Staphylococcus aureus		*Enterococcus faecalis*		*Escherichia coli*		*Pseudomonas aeruginosa*	
	MIC	MBC	MIC	MBC	MIC	MBC	MIC	MBC
AgNP (6 days)	> 2.5	> 2.5	> 2.5	> 2.5	1.25	1.25	2.5	2.5
AgNP (9 days)	> 2.5	> 2.5	> 2.5	> 2.5	0.62	0.62	0.62	0.62
AgNP (12 days)	> 2.5	> 2.5	> 2.5	> 2.5	> 2.5	> 2.5	> 2.5	> 2.5

The TEM image suggests that the particles are poly dispersed and were round in shape (Fig. 7), next features found by Ammar and El-Desouky (2016) that in their study revealed that the size of AgNPs ranged between 14 and 25 nm in the case of *P. expansum* and 10–18 nm in the case of *A. terreus*.

Antibacterial tests

The MBC results show that all the concentrations with bactericidal activity prevented bacterial growth in the Petri dish and the MIC values were the same and resulted that the nanoparticles had bactericidal activity (Table 2). The MBC and MIC values were lower for Gram-negative (*E. coli* and *P. aeruginosa*) than for Gram-positive (*S. aureus* and *E. faecalis*) bacteria and this difference is attributed to the bacterial cell wall structure, which in Gram-negative bacteria is formed by a thin peptidoglycan layer (2–3 nm) between the cytoplasmic membrane and the outer membrane. Gram-positive bacteria do not have the outer membrane; however, their cell wall is formed by a thicker peptidoglycan layer (~ 30 nm) bond to short peptides, forming a rigid structure that hinders the impregnation of AgNP (Bezerra 2015).

The antimicrobial potential of Ag^+ ions is related to their positive charge, in this way, Gram-positive microorganisms may be less susceptible to their action than the Gram-negative ones, due to the electrical charge attributed to the peptidoglycan molecules being negative, these ions tend to remain attached to this structure and not carry out its action (Sharma et al. 2009; Ahmed et al. 2016).

The bacterial membrane is a crucial structure for the action of AgNP. These particles manage to change the *cis/trans* ratio of unsaturated fatty acids and interact with proteins through redox reactions forming electron donor complexes containing oxygen, phosphor, nitrogen or sulfur atoms. These mechanisms can change the membrane fluidity, inactivate proteins, increase its permeability and eventually result in loss of integrity, which can explain the best antibacterial activities from AgNP against Gram-negative strains—mostly for 9 days AgNP (0.62). Regarding the loss of activity observed for 12 days nanoparticles (> 2.5), it is due to the particles degradation (Durán et al. 2016).

Among the mechanisms responsible for the antibacterial activity attributed to AgNP we can highlight their propensity to accumulate in the membrane and causing damage to the cell wall or cell membranes of the bacteria because the silver atoms irreversibly bind the thiol groups of enzymes with stable bonds compromising the activity of enzymes in trans membrane energy generation or in ionic transport (Gupta et al. 1988). In addition to its interference in cell division by breaking the bonds between the pairs of nitrogenous bases resulting in marked enhancement of pyrimidine dimerization by photodynamic reaction and impairs on DNA replication (Fox and Modak 1974; Ahmed et al. 2016).

Conclusions

Among the four isolates of Amazon fungi chosen for the study (TCH 01, TCH 02, TCH 03 and TCH 06) only the TCH 01 (from soil) was able to biosynthesize the AgNP, evidenced by the RPSL band, a key feature for the characterization of AgNP in UV–Vis analysis. Through tests of pH variation and reaction time, it was found that when the TCH 01 isolate was cultivated at pH 5 over 9 days, resulted in smaller nanoparticles

sizes and the better polydispersity indexes. For the zeta potential, all AgNP presented incipient instability.

The AgNP biosynthesized by the TCH 01 isolate had antibacterial activity against Gram-negative bacteria and this ability adds value to the Amazon fungus TCH 01 (*Trichoderma* sp.), by showing its potential for biotechnology and chemical and pharmaceutical industries. This study took a further step towards an eco-friendly synthesis of AgNP; however, further studies will be needed to assess its applicability in pharmaceutical formulations for bactericidal purposes.

Compliance with ethical standards

Conflict of interest The authors declare that they have no conflict of interest.

References

Abdelrahim K, Mahmoud SY, Ali AM, Almaary KS, Mustafa AE-ZMA, Husseiny SM (2017) Extracellular biosynthesis of silver nanoparticles using *Rhizopus stolonifer*. Saudi J Biol Sci 24:208–216

Ahluwalia V, Kumar J, Sisodia R, Shakil NA, Suresh W (2014) Green synthesis of silver nanoparticles by *Trichoderma harzianum* and their bio-efficacy evaluation against *Staphylococcus aureus* and *Klebsiella pneumonia*. Ind Crops Prod 55:202–206

Ahmed S, Ahmad M, Swami BL, Ikram S (2016) A review on plants extract mediated synthesis of silver nanoparticles for antimicrobial applications: a green expertise. J Adv Res 7:17–28

Almeida ES (2017) Biossíntese e caracterização de nanopartículas de prata por fusarium oxysporum. Universidade Federal de Santa Catarina, Santa Catarina

Ammar HS, El-Desouky TA (2016) Green syntehsis of nanosilver by *Aspergillius terreus* HA1N and *Penicillium expansum* HA2N and its antifungal activity against mycotoxigenic fungi. J Appl Microbiol 121:89–100

Balakrishnan RM (2014) Biosynthesis and optimization of silver nanoparticles by endophytic fungus *Fusarium solani*. Mater Lett 132:428–431

Bezerra AVA (2015) Síntese, caracterização de nanopartículas de prata e avaliação da atividade biocida em filmes de poliestireno. Universidade Federal de Santa Catarina, Florianópolis

Birolli WG, Ferrreira IM, Jimenez DEQ, Silva BNM, Silva BV, Pinto AC, Porto ALM (2017) First asymmetric reduction of isatin by marine-derived fungi. J Braz Chem Soc 28:1023–1029

Cardoso CO (2017) Avaliação da penetração da oxaliplatina na mucosa oral a partir de nanopartículas de quitosana. Universidade Federal de Brasília, Brasília

Cavalcante BN (2014) Atividade antibacteriana e antifúngica de nanopartículas de prata produzidas por Curvularia inaequalis (Shear) Boedijn. Universidade do Vale do São Francisco, Petrolina

Chen H, Mothapo NV, Shi W (2015) Soil moisture and pH control relative contributions of fungi and bacteria to N_2O production. Microb Ecol 69:180–191

Clinical and Laboratory Standards Institute (2012) Methods for dilution antimicrobial susceptibility tests for bacteria that grow aerobically. ISBN 1-56238-783-9.

Durán N, Durán M, De Jesus MB, Seabra AB, Fávaro WJ, Nakazato G (2016) Silver nanoparticles: a new view on mechanistic aspects on antimicrobial activity. Nanomedicine 12:789–799

Edwards B (2017) Silver nanoparticles: advances in research and applications. Nova Science Publishers Inc., Hauppauge

Elgorban AM, Al-Rahmah AN, Sayed SR, Hirad A, Mostafa AA-F, Bahkali AH (2016) Antimicrobial activity and green synthesis of silver nanoparticles using *Trichoderma viride*. Biotechnol Biotechnol Equip 30:299–304

Ferreira IM, Meira EB, Rosset IG, Porto ALM (2015) Chemoselective biohydrogenation of α,β- and α,β,γ,δ-unsaturated ketones by the marine-derived fungus *Penicillium citrinum* CBMAI 1186 in a biphasic system. J Mol Catal B Enzym 115:59–65

Fox CL Jr, Modak SM (1974) Mechanism of silver sulfadiazine action on burn wound infections. Antimicrob Agents Chemother 5:582–588

Freitas LMC, Barbosa BCA, Rodrigues K, Marinho G (2017) Emprego de *Aspergillus niger* AN 400 em reatores de bancada para remover pesticida de matriz aquosa. Engenharia Sanitaria e Ambiental 22:1175–1185

Gaikwad SC, Birla SS, Ingle AP, Gade AK, Marcato PD, Rai M, Duran N (2013) Screening of different. J Braz Chem Soc 00:1–9

Ghiuță I, Cristea D, Munteanu D (2017) Synthesis methods of metallic nanoparticles: an overview. Bull Trans Univ Bras Series I 10:133–140

Gupta A, Maynes M, Silver S (1988) Effects of halides on plasmid-mediated silver resistance in *Escherichia coli*. Appl Environ Microbiol 64:5042–5045

Hargreaves PI, Pereira Jr N (2008) Bioprospecção de novas celulases de fungos provenientes da floresta amazônica e otimização de sua produção sobre celulignina de bagaço de cana. Universidade Federal do Rio de Janeiro, Rio de Janeiro

Holanda FH, Birolli WG, Morais ES, Sena IS, Ferreira AM, Faustino SMM, Solon LCS, Porto ALM, Ferreira IM (2019) Study of biodegradation of chloramphenicol by endophytic fungi isolated from *Bertholletia excelsa* (Brazil nuts). Biocatal Agric Biotechnol 20:101200–101208

Ilaria A, Kenny J (2013) Silver nanoparticles: synthesis, uses and health concerns. Nova Science Publishers Inc., Hauppauge

Kelly TJ, Lawson IT, Roucoux KH, Baker TR, Jones TD, Sanderson NK (2017) The vegetation history of an Amazonian domed peatland. Palaeogeogr Palaeoclimatol Palaeoecol 468:129–141

Ko S, Huh C (2019) Use of nanoparticles for oil production applications. J Petrol Sci Eng 172:97–114

Liu J, Jiang G (2015) Silver nanoparticles in the environment. Springer, Berlin

Marinho G, Freitas LMC, Barbosa BCA, Rodrigues KDA (2017) Employment of *Aspergillus niger* AN 400 in batch reactors to remove pesticide aqueous matrix. Eng San e Amb 22:1175–1185

McShan D, Zhang Y, Deng H, Ray PC, Yu H (2015) Synergistic antibacterial effect of silver nanoparticles combined with ineffective antibiotics on drug resistant *Salmonella typhimurium* DT104. J Env Sci and Health, Part C 33:369–384

Mikolajczyk A, Gajewicz A, Rasulev B, Schaeublin N, Maurer-Gardner E, Hussain S, Leszczynski J, Puzyn T (2015) Zeta potential for metal oxide nanoparticles: a predictive model developed by a nano-quantitative structure–property relationship approach. Chem Mater 27:2400–2407

Mishra A, Kumari M, Pandey S, Chaudhry V, Gupta KC, Nautiyal CS (2014) Biocatalytic and antimicrobial activities of gold nanoparticles synthesized by *Trichoderma* sp. Bioresour Technol 166:235–242

Neethu S, Midhun SJ, Radhakrishnan EK, Jyothis M (2018) Green synthesized silver nanoparticles by marine endophytic fungus *Penicillium polonicum* and its antibacterial efficacy against biofilm forming, multidrug-resistant *Acinetobacter baumanii*. Micro Pathog 116:263–272

Pathma J, Sakthivel N (2012) Microbial diversity of vermicompost bacteria that exhibit useful agricultural traits and waste management potential. SpringerPlus 1:26–26

Ravindran A, Chandran P, Khan SS (2013) Biofunctionalized silver nanoparticles: advances and prospects. Colloids Surf B 105:342–352

Sajanlal PR, Sreeprasad TS, Samal AK, Pradeep T (2011) Anisotropic nanomaterials: structure, growth, assembly, and functions. Nano rev 2:1–62

Shah M, Fawcett D, Sharma S, Tripathy KS, Poinern EG (2015) Green synthesis of metallic nanoparticles via biological entities. Materials 8:7278–7308

Sharma VK, Yngard RA, Lin Y (2009) Silver nanoparticles: green synthesis and their antimicrobial activities. Adv Coll Interface Sci 145:83–96

Wei L, Lu J, Xu H, Patel A, Chen Z-S, Chen G (2015) Silver nanoparticles: synthesis, properties, and therapeutic applications. Drug Discov Today 20:595–601

Welles AE (2010) Silver nanoparticles: properties, characterization and applications. Nova Science Publishers, New York

Zhang X-F, Liu Z-G, Shen W, Gurunathan S (2016) Silver nanoparticles: synthesis, characterization, properties, applications, and therapeutic approaches. Int J Mol Sci 17:1–34